

MHD Turbulent Flow in a Porous Medium with Hall Currents, Joule's Heating and Mass Transfer

Job Oqhoyho Mayaka¹, Johana Sigey², Mathew Kinyanjui³

¹Pan African University Institute of Basic Sciences, Technology and Innovation
Department of Mathematics, P.O. Box 62000-00200, Nairobi, Kenya

²Jomo Kenyatta University of Agriculture and Technology
School of Mathematics, Pure and Applied Mathematics Department, P.O. Box 62000-00200, Nairobi, Kenya

³Jomo Kenyatta University of Agriculture and Technology
School of Mathematics, Pure and Applied Mathematics Department, P.O. Box 62000-00200, Nairobi, Kenya

Abstract: *The MHD turbulent flow past a porous vertical plate is solved using FTCS finite difference method. Turbulence is treated using Prandtl's mixed lengths theorem. Factored into the model are mass transfer, Hall currents and Joule's heating. All these factors are found to have a profound effect on the primary and secondary velocity profiles, temperature profiles and concentration profiles.*

Keywords: MHD, Hall currents, Joule's heating, FTCS, Prandtl mixed lengths theorem

1. Introduction

While electromagnetism majorly deals with conducting solids, the study of the flow of conducting fluids defines a different field called magnetohydrodynamics (MHD). Such flows are important in that they find applications in MHD generators, liquid metal levitation and as a basis for plasma studies.

The study of MHD can be traced back to Faraday's experiment to determine the current generated by the flow of River Thames in the earth's magnetic field. It was the effort of Prandtl [1] that unified the engineering fluid dynamics experiments and the theory by introducing the boundary layer theory. Hartmann [2] then engineered the Hartmann pump and described the theory of mercury dynamics. The desire to understand the sustenance of the geomagnetic field led to the development of more theories. However, it was Alfven's [3] frozen field theory that revolutionized the study of MHD.

Later, Hasimoto [4] studied boundary layer growth on a flat plate with uniform suction or injection. Following this Gupta and Soundalgekar [5] studied the hydromagnetic flow and heat transfer in an infinite plate past a rotating porous wall. Then Mansuti et al [6] discussed the steady flow of a non-Newtonian fluid past a porous plate with suction or injection. Kinyanjui et al [7] followed this with the study of the Stoke's problem of convective flow from a vertical infinite plate in a rotating fluid. Sharma and Pareek [8] then explained the behaviour of steady free convective MHD flow past a vertical porous moving surface. Kwanza et al [9] analyzed MHD Stokes free convection flow past an infinite vertical porous plate subjected to constant heat flux with ion slip current and radiation absorption. Following these, Makinde et al [10] discussed the unsteady free convective flow with suction on an accelerating porous plate. Chaudhary [11] carried out studies on combined heat and mass transfer effects on MHD free convection flow past an oscillating plate imbedded in porous medium. Das et al [12] followed

this up with a numerical investigation of the unsteady free convective flow past an accelerated vertical porous plate with suction and heat flux. Then Ghosh and Ghosh [13] studied the hydromagnetic rotating flow of a dusty fluid near a pulsating plate with several limiting case studies. Das et al [14] followed up their earlier work by studying the mass transfer effects on unsteady hydromagnetic convective flow past a vertical porous plate in a porous medium with heat source. Lately, Mutua et al [15] studied the Stokes problem of a free convective flow past a vertical infinite plate in a rotating fluid with hall currents in the presence of a variable magnetic field.

MHD is an active field and there are many studies that have been carried out and are still being carried out. The present study is based on the works of Das et al [14] and Mutua et al [15]. A combination the rotation and mass transfer effects studied by the two has been sought in the present paper.

2. Geometry of the Flow Problem

The fluid is assumed to flow in the x and z -plane with velocities U and W , respectively. A strong constant magnetic field H_0 is applied along the y -direction. The fluid is in a constant rotation with velocity, Ω . A porous plate in the xz plane is initially in a rigid body rotation with the fluid. The temperature on the plate is initially instantaneously raised to T_w and the vertical velocity is also instantaneously raised W_o . A drift velocity u_0 due to injection or suction is implied. The concentration at the plate is instantaneously set to C_w . The effect of these changes is studied with time within the boundary layer of the fluid. Figure 1 summarizes the problem specification.

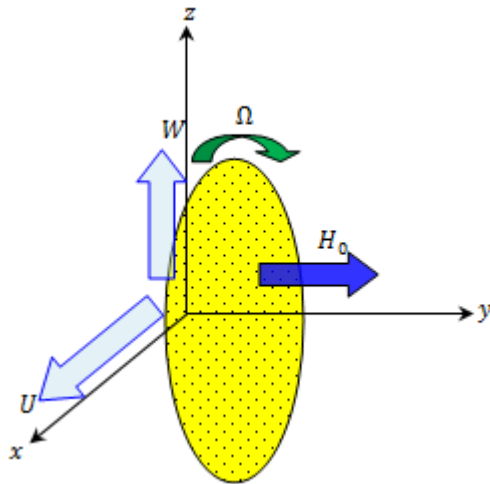


Figure 1: A diagrammatic representation of the MHD problem

3. Mathematical Formulation

3.1 General Governing Equations

Considering an incompressible fluid with steady flow the equation of continuity reduces to:

$$\nabla \cdot \mathbf{V} = 0 \quad (1)$$

The momentum equation taking into account the body forces and the surface forces is given as:

$$\rho \left(\frac{\partial \mathbf{V}}{\partial t} + \mathbf{V} \cdot \nabla \mathbf{V} \right) = \rho \mathbf{g} + \rho_q \mathbf{E} + \mathbf{J} \times \mathbf{B} - \nabla p + \mu \nabla^2 \mathbf{V} \quad (2)$$

The electrostatic force $\rho_q \mathbf{E}$ is negligibly small when compared to the Lorentz force, $\mathbf{J} \times \mathbf{B}$, and can thus be omitted from equation (2). This together with the Coriolis's force, $-2\boldsymbol{\Omega} \times \mathbf{V}$, due to rotation, results in the momentum equation as:

$$\rho \left(\frac{\partial \mathbf{V}}{\partial t} + \mathbf{V} \cdot \nabla \mathbf{V} + 2\boldsymbol{\Omega} \times \mathbf{V} \right) = \rho \mathbf{g} + \mathbf{J} \times \mathbf{B} + \dots - \nabla p + \mu \nabla^2 \mathbf{V} \quad (3)$$

The energy equation is the conduction equation taking into account viscous dissipation and Joule's heating. This is given as:

$$\rho C_p \left(\frac{\partial T}{\partial t} + \mathbf{V} \cdot \nabla T \right) = k \nabla^2 T + \underbrace{\mathbf{\Pi} : \nabla \mathbf{V}}_{\text{Viscous dissipation}} + \dots + \underbrace{\frac{J^2}{\sigma}}_{\text{Joule's heating}} \quad (4)$$

The mass transfer equation is a diffusion equation given as:

$$\frac{\partial C}{\partial t} + \mathbf{V} \cdot \nabla C = D \nabla^2 C \quad (5)$$

3.2 Component Form of the Governing Equations

Equations (1), (3), (4) and (5) are in vector form. Upon solving the components of the vectors, we have the

continuity equation reducing to:

$$\frac{\partial u}{\partial x} = \frac{\partial w}{\partial z} = 0 \quad (6)$$

Using the Boussinesq's approximation taking the thermal and concentration coefficients of expansion, the momentum equation in component form becomes:

$$\begin{aligned} \frac{\partial u}{\partial t} + 2\Omega w &= \frac{-B_0 J_z}{\rho} + \nu \frac{\partial^2 u}{\partial y^2} \\ \frac{\partial w}{\partial t} - 2\Omega u &= \frac{B_0 J_x}{\rho} + g \left[\beta (T - T_\infty) + \beta_c (C - C_\infty) \right] \\ &\quad + \nu \frac{\partial^2 w}{\partial y^2} \end{aligned} \quad (7)$$

In the pair of equations (7) the momentum equation split to give the two components of velocity being the primary, w , and the secondary, u , velocities.

Solving the component form of the energy equation yields:

$$\begin{aligned} \rho C_p \frac{\partial T}{\partial t} &= k \frac{\partial^2 T}{\partial y^2} + \mu \left[\left(\frac{\partial u}{\partial y} \right)^2 + \left(\frac{\partial w}{\partial y} \right)^2 \right] \dots \\ &\quad + \frac{1}{\sigma} (J_x^2 + J_z^2) \end{aligned} \quad (8)$$

The mass transfer equation, upon solving the component form, becomes:

$$\frac{\partial C}{\partial t} = D \frac{\partial^2 C}{\partial y^2} \quad (9)$$

3.3 Turbulence Effects

Although there are many approaches to handle turbulence, the Reynold's Averaged Navier Stokes (RANS) approach is the easiest to employ in computation (Del Sordo *et al* [16]). In this approach a flow variable, say, ξ , is broken as:

$$\xi = \bar{\xi} + \xi' \quad (10)$$

Where $\bar{\xi}$ is the time averaged variable while ξ' is the perturbation from the average value.

Employing the RANS approach, the equation of continuity decomposes into:

$$\frac{\partial \bar{u}}{\partial x} = \frac{\partial \bar{w}}{\partial z} = 0 \quad (11)$$

When the same averaging is used together with Prandtl mixing length hypothesis (McComb [17]) the two components of velocity are obtained as:

$$\begin{aligned} \frac{\partial \bar{u}}{\partial t} + \bar{v} \frac{\partial \bar{u}}{\partial y} + 2\Omega \bar{w} &= \frac{-B_0 J_z}{\rho} + \nu \frac{\partial^2 \bar{u}}{\partial y^2} + \\ &2\kappa^2 \left[y \left(\frac{\partial \bar{u}}{\partial y} \right)^2 + y^2 \left(\frac{\partial \bar{u}}{\partial y} \right) \left(\frac{\partial^2 \bar{u}}{\partial y^2} \right) \right] \\ \frac{\partial \bar{w}}{\partial t} + \bar{v} \frac{\partial \bar{w}}{\partial y} - 2\Omega \bar{u} &= \frac{B_0 J_x}{\rho} + \\ &g \left[\beta (T - T_\infty) + \beta_c (C - C_\infty) \right] + \nu \frac{\partial^2 \bar{w}}{\partial y^2} \\ &+ 2\kappa^2 \left[y \left(\frac{\partial \bar{w}}{\partial y} \right)^2 + y^2 \left(\frac{\partial \bar{w}}{\partial y} \right) \left(\frac{\partial^2 \bar{w}}{\partial y^2} \right) \right] \end{aligned} \quad (12)$$

When turbulence is factored into equation (8), the energy equation becomes:

$$\begin{aligned} \rho C_p \left(\frac{\partial T}{\partial t} + \bar{v} \frac{\partial T}{\partial y} \right) &= k \frac{\partial^2 T}{\partial y^2} + \\ &\mu \left[\left(\frac{\partial \bar{u}}{\partial y} \right)^2 + \left(\frac{\partial \bar{w}}{\partial y} \right)^2 \right] + \frac{1}{\sigma} (J_x^2 + J_z^2) \end{aligned} \quad (13)$$

Employing the RANS method to the mass transfer equation (9) yields:

$$\frac{\partial C}{\partial t} + \bar{v} \frac{\partial C}{\partial y} = D \frac{\partial^2 C}{\partial y^2} \quad (14)$$

3.4 Hall Current Effect

The Generalized Ohm's law with Hall currents, ion slip currents and electron pressure gradient is given as:

$$\begin{aligned} \mathbf{J} + \frac{\omega_e \tau_e}{|\mathbf{B}|} \left(1 - \frac{\omega_i \tau_i}{|\mathbf{B}|} \right) (\mathbf{J} \times \mathbf{B}) \\ = \sigma \left(\mathbf{E} + \mathbf{V} \times \mathbf{B} - \frac{1}{ne} \nabla p_e \right) \left(1 - \frac{1}{2} \frac{V^2}{c^2} + \dots \right) \end{aligned} \quad (15)$$

Since $V \ll c \Rightarrow \frac{1}{2} \frac{V^2}{c^2} \ll 1$, the last parenthesis term reduces to 1. The problem is a short circuit one and hence the implied electric field, $\mathbf{E} = 0$. Also the ion slip current term, $\frac{\omega_i \tau_i}{|\mathbf{B}|} \ll 1$. With these estimations equation (15) simplifies to:

$$\mathbf{J} + \frac{\omega_e \tau_e}{H_0} (\mathbf{J} \times \mathbf{H}) = \sigma \mu_e \mathbf{V} \times \mathbf{H} \quad (16)$$

In equation (16) above we used the definition $\mathbf{B} = \mu_e \mathbf{H}$ and hence $|\mathbf{B}| = B_0 = \mu_e H_0$.

Solution of the component form of equation (16) results in the two components of current as:

$$\begin{aligned} J_x &= \frac{\sigma \mu_e H_0}{1 + m^2} (mu - w) \\ J_z &= \frac{\sigma \mu_e H_0}{1 + m^2} (mw + u) \end{aligned} \quad (17)$$

The Hall currents affect the pair of continuity equations (12) and the energy equation (13). Putting relations (17) into the two equations yields:

$$\begin{aligned} \frac{\partial \bar{u}}{\partial t} + \bar{v} \frac{\partial \bar{u}}{\partial y} + 2\Omega \bar{w} &= \frac{-\sigma \mu_e^2 H_0^2}{\rho (1 + m^2)} (m\bar{w} + \bar{u}) + \\ &\nu \frac{\partial^2 \bar{u}}{\partial y^2} + 2\kappa^2 \left[y \left(\frac{\partial \bar{u}}{\partial y} \right)^2 + y^2 \left(\frac{\partial \bar{u}}{\partial y} \right) \left(\frac{\partial^2 \bar{u}}{\partial y^2} \right) \right] \\ \frac{\partial \bar{w}}{\partial t} + \bar{v} \frac{\partial \bar{w}}{\partial y} - 2\Omega \bar{u} &= \frac{\sigma \mu_e^2 H_0^2}{\rho (1 + m^2)} (m\bar{u} - \bar{w}) + \\ &g \left[\beta (T - T_\infty) + \beta_c (C - C_\infty) \right] + \nu \frac{\partial^2 \bar{w}}{\partial y^2} + \\ &2\kappa^2 \left[y \left(\frac{\partial \bar{w}}{\partial y} \right)^2 + y^2 \left(\frac{\partial \bar{w}}{\partial y} \right) \left(\frac{\partial^2 \bar{w}}{\partial y^2} \right) \right] \end{aligned} \quad (18)$$

and

$$\begin{aligned} \rho C_p \left(\frac{\partial T}{\partial t} + \bar{v} \frac{\partial T}{\partial y} \right) &= k \frac{\partial^2 T}{\partial y^2} + \\ &\mu \left[\left(\frac{\partial \bar{u}}{\partial y} \right)^2 + \left(\frac{\partial \bar{w}}{\partial y} \right)^2 \right] + \\ &\frac{\sigma \mu_e^2 H_0^2}{(1 + m^2)^2} \left[(m\bar{u} - \bar{w})^2 + (m\bar{w} + \bar{u})^2 \right] \end{aligned} \quad (19)$$

3.5 Non-Dimensionalization

The dimensional form of equations (11), (18), (19) and (14), which are, respectively, the equation of continuity, equation of momentum, equation of energy and equation of mass transfer is obtained by replacing every flow variable, ξ with ξ^* . The bars above some of the variables are neglected.

These variables are t, y, u, w, T and C . The dimensional initial and boundary conditions are given as:

$$\begin{aligned} t^* < 0: & \left. \begin{aligned} u^* &= 0, w^* = 0, T^* = T_\infty^*, \\ C^* &= C_\infty^* \end{aligned} \right\| \text{Everywhere} \\ t^* \geq 0: & \left. \begin{aligned} u^* &= U_0, w^* = W_0, T^* = T_w^*, \\ C^* &= C_w^* \end{aligned} \right\| \text{At } y = 0 \quad (20) \\ & \left. \begin{aligned} u^* &\rightarrow 0, w^* \rightarrow 0, T^* \rightarrow T_\infty^*, \\ C^* &\rightarrow C_\infty^* \end{aligned} \right\| \text{As } y \rightarrow \infty \end{aligned}$$

We define the following non-dimensional variables:

$$\begin{aligned} t &= \frac{t^* U^2}{\nu}, y = \frac{y^* U}{\nu}, u = \frac{u^*}{U}, v_0 = \frac{v_0^*}{U}, w = \frac{w^*}{U}, \\ \theta &= \frac{T^* - T_\infty^*}{T_w^* - T_\infty^*}, C = \frac{C^* - C_\infty^*}{C_w^* - C_\infty^*} \end{aligned} \quad (21)$$

We also define the following useful non-dimensional numbers and parameters for the present problem.

$$\begin{aligned} Pr &= \frac{\mu C_p}{k}, Gr_L = \frac{\nu g \beta (T_w - T_\infty)}{U^3}, \\ Gr_C &= \frac{\nu g \beta_C (T_w - T_\infty)}{U^3}, Ec = \frac{U^2}{C_p (T_w - T_\infty)}, \\ Sc &= \frac{\nu}{D}, M^2 = \frac{\sigma \mu_e^2 H_0^2 \nu}{\rho U^2}, Er = \frac{\Omega \nu}{U^2} \end{aligned} \quad (22)$$

Using (21) we reduce the dimensional equations into non-dimensional form. Further simplification is obtained by using the relations (22). We then end up with the final set of equations as:

$$\begin{aligned} \frac{\partial u}{\partial t} + v_0 \frac{\partial u}{\partial y} + 2Erw &= -\frac{M^2}{1+m^2} (mw + u) + \frac{\partial^2 u}{\partial y^2} + \\ & 2\kappa^2 \left[y \left(\frac{\partial u}{\partial y} \right)^2 + y^2 \left(\frac{\partial u}{\partial y} \right) \left(\frac{\partial^2 u}{\partial y^2} \right) \right] \\ \frac{\partial w}{\partial t} + v_0 \frac{\partial w}{\partial y} - 2Eru &= \frac{M^2}{1+m^2} (mu - w) + \\ & [Gr_L \theta + Gr_C C] + \frac{\partial^2 w}{\partial y^2} + \\ & 2\kappa^2 \left[y \left(\frac{\partial w}{\partial y} \right)^2 + y^2 \left(\frac{\partial w}{\partial y} \right) \left(\frac{\partial^2 w}{\partial y^2} \right) \right] \end{aligned} \quad (23)$$

$$\begin{aligned} \frac{\partial \theta}{\partial t} + v_0 \frac{\partial \theta}{\partial y} &= \frac{1}{Pr} \frac{\partial^2 \theta}{\partial y^2} + Ec \left[\left(\frac{\partial u}{\partial y} \right)^2 + \left(\frac{\partial w}{\partial y} \right)^2 \right] \\ & + \frac{Ec M^2}{(1+m^2)^2} [(mu - w)^2 + (mw + u)^2] \end{aligned} \quad (24)$$

$$\frac{\partial C}{\partial t} + v_0 \frac{\partial C}{\partial y} = \frac{1}{Sc} \frac{\partial^2 C}{\partial y^2} \quad (25)$$

Equations (23), (24) and (25) are the final set of non-dimensional governing equations for secondary velocity, u , primary velocity, w , temperature, θ and concentration, C . The corresponding set of non-dimensional boundary conditions is:

$$\begin{aligned} t < 0: & U = 0, W = 0, \theta = 0, C = 0 \text{ everywhere} \\ t \geq 0: & U = 0, W = 1, \theta = 1, C = 1 \text{ at } y = 0 \\ & : U \rightarrow 0, V \rightarrow 0, \theta \rightarrow 0, C \rightarrow 0 \text{ as } y \rightarrow \infty \end{aligned} \quad (26)$$

4. Numerical Method

Equations (23), (24) and (25) are highly coupled and non-linear. Obtaining a closed form of the solutions to such type of equations is difficult. With the help of the boundary conditions (26) it is possible to set up numerical solutions. Since all the flow variables are functions of y and t , a two dimensional grid was set up. A finite difference method (FDM) was used to solve the MHD problem at the set grid points. The forward time central space (FTCS) model was used to solve the final set of equations. This is because other FDM methods are very difficult to use for such highly coupled and non-linear set of partial differential equations.

The resulting set of difference equations for the primary velocity, secondary velocity, temperature and concentration is respectively:

$$w_j^{k+1} = w_j^k - \frac{v_0 r_1}{2} (w_{j+1}^k - w_{j-1}^k) + 2Er\Delta t u_j^k + \frac{M^2 \Delta t}{1+m^2} (mu_j^k + w_j^k) + \Delta t (Gr_L \theta_j^k + Gr_C C_j^k) + r_2 (w_{j+1}^k - 2w_j^k - w_{j-1}^k) + 2\kappa^2 \left[\frac{r_2}{4} (y_j) (w_{j+1}^k - w_{j-1}^k)^2 + \frac{r_3}{2} (y_j)^2 (w_{j+1}^k - w_{j-1}^k) (w_{j+1}^k - 2w_j^k - w_{j-1}^k) \right] \quad (27)$$

$$u_j^{k+1} = u_j^k - \frac{v_0 r_1}{2} (u_{j+1}^k - u_{j-1}^k) - 2Er\Delta t w_j^k - \frac{M^2 \Delta t}{1+m^2} (mw_j^k + u_j^k) + r_2 (u_{j+1}^k - 2u_j^k - u_{j-1}^k) + 2\kappa^2 \left[\frac{r_2}{4} (y_j) (u_{j+1}^k - u_{j-1}^k)^2 + \frac{r_3}{2} (y_j)^2 (u_{j+1}^k - u_{j-1}^k) (u_{j+1}^k - 2u_j^k - u_{j-1}^k) \right] \quad (28)$$

$$\theta_j^{k+1} = \theta_j^k - \frac{v_0 r_1}{2} (\theta_{j+1}^k - \theta_{j-1}^k) + \frac{r_2}{Pr} (\theta_{j+1}^k - 2\theta_j^k - \theta_{j-1}^k) + \frac{Ecr_2}{4} [(u_{j+1}^k - u_{j-1}^k)^2 + (w_{j+1}^k - w_{j-1}^k)^2] + \frac{EcM^2 \Delta t}{(1+m^2)^2} [(mu_j^k - w_j^k)^2 + (mw_j^k + u_j^k)^2] \quad (29)$$

$$C_j^{k+1} = C_j^k - \frac{v_0 r_1}{2} (C_{j+1}^k - C_{j-1}^k) + \frac{r_2}{Sc} (C_{j+1}^k - 2C_j^k - C_{j-1}^k) \quad (30)$$

In the relations (27), (28), (29) and (30) we made use of the substitution $r_1 = \frac{\Delta t}{\Delta y}$, $r_2 = \frac{\Delta t}{(\Delta y)^2}$ and $r_3 = \frac{\Delta t}{(\Delta y)^3}$.

Although the spatial dimensions are to run to infinity, within the time of observation $y = 4$ was chosen as the limit of the boundary layer. The time of observation was limited to unit.

Although the algorithm for the FTCS is relatively easy to formulate, it requires many more grid points for accurate results. The more the number of grid points the lengthier the computation required. A computer program in matlab was developed to solve the difference equations above.

5. Results and Discussions

The three dimensional mesh plots generated (Figure 2) show the decay of the primary velocity, temperature and concentration profiles along the y and t axes. The growth, then decay of the secondary velocity is also observed. This is in agreement with the boundary conditions and the general trend of the transfer of the wall properties into the boundary layer. We next vary each fluid property while maintaining the other properties at their default values and observe the effect on the four flow variables. The default values are:

$$Pr = 0.71, \quad Gr_L = 1, \quad Gr_C = 1, \quad Ec = 1, \quad Sc = 2.5, \\ M^2 = 1, \quad m = 0.1, \quad Er = 1 \quad \text{and} \quad v_0 = 0.5$$

The effect of the Prandtl number, Pr , is reflected in **Error! Reference source not found.** It accelerates both the primary velocity and secondary velocities. Temperature decreases with increase in Prandtl number since this leads to a smaller temperature boundary layer relative to momentum boundary layer.

The thermal variant of the Grashof number, Gr_L , generally enhances both primary and secondary velocities but has a diminished effect on the temperature profiles (Figure 4). The concentration variant of the Grashof number, Gr_C , has a similar effect to that of the thermal variant (Figure 5). The Grashof numbers generally enhance buoyancy and hence velocity.

The Eckert number, Ec , has a very slight effect on both primary and secondary velocity but a more appreciable advancing effect on the temperature profiles (Figure 6). The Eckert number implies increased kinetic energy and less enthalpy, hence the accelerating effect on temperature. The Schmidt number, Sc , diminishingly affects mostly the concentration profiles (Figure 7). Increased Schmidt numbers imply less mass diffusivity and hence the decline in concentration profiles.

The magnetic parameter, M^2 , decreases both primary and secondary velocities due to retarding effect of the Lorentz force but increases the temperature profiles due to Joule's resistive heating (Figure 8). The Hall parameter, m , slightly enhances both primary and secondary velocities due to the cyclotron effect (Figure 9).

The rotational parameter, Er , interestingly diminishes the primary velocity profiles while accelerating the secondary velocity profiles (Figure 10). This is due to the rotational transfer of magnitude from the primary to the secondary velocity. The slight temperature increase is attributed to the increased turbulence due to rotation.

Lastly, the mass transfer velocity, v_0 , accelerates all the flow variables (Figure 11). This is because increased injection rates enhance transfer from the plate to the rest of the fluid which leads to enhanced boundary layers.

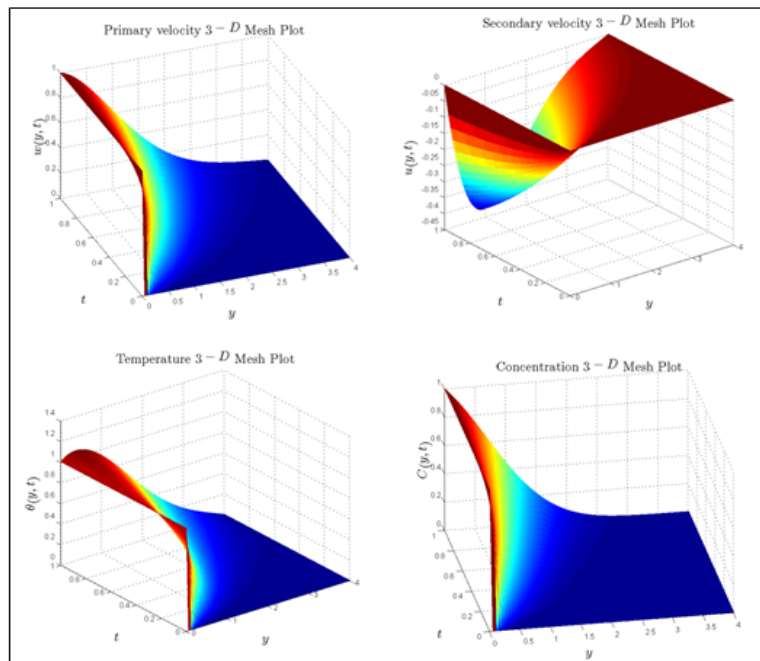


Figure 2: Three dimensional mesh plots for the four flow variables

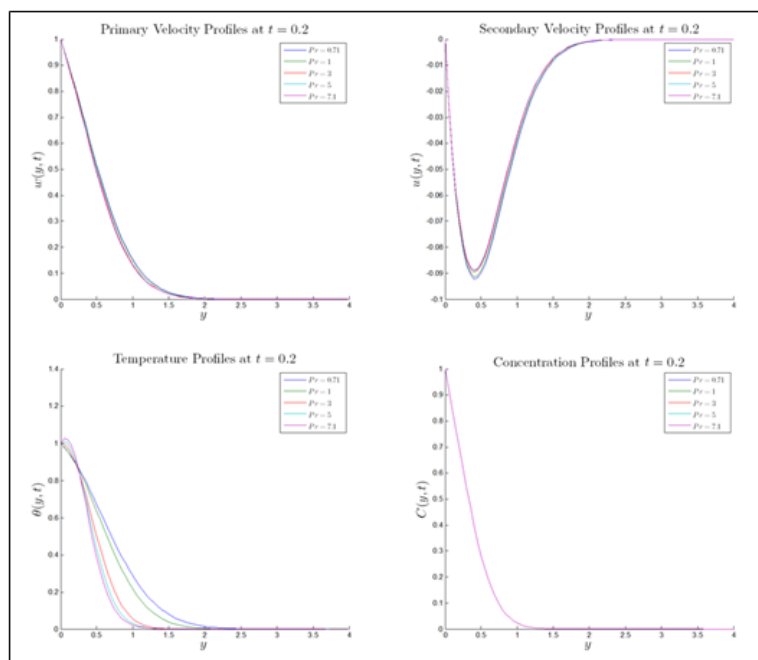


Figure 3: Fluid flow profiles for various Prandtl numbers

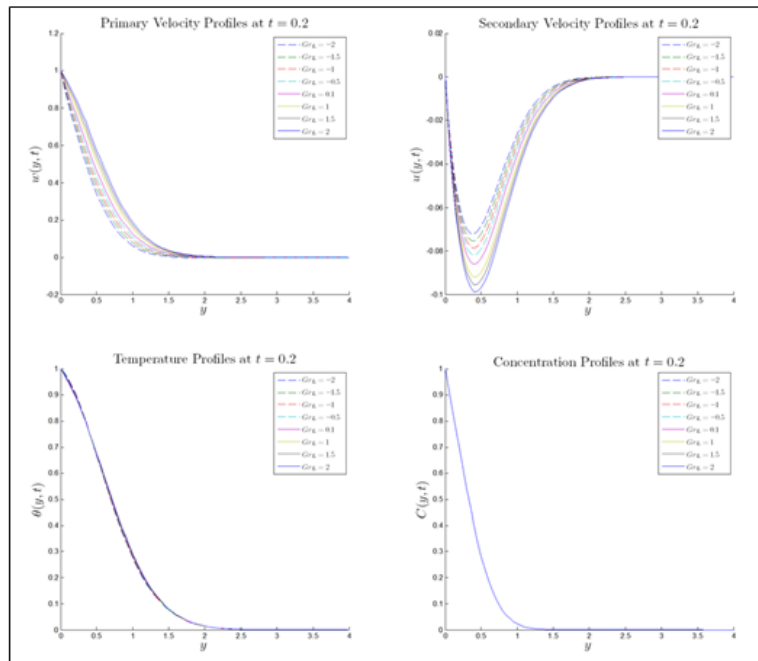


Figure 4: Fluid flow profiles for various thermal Grashof numbers.

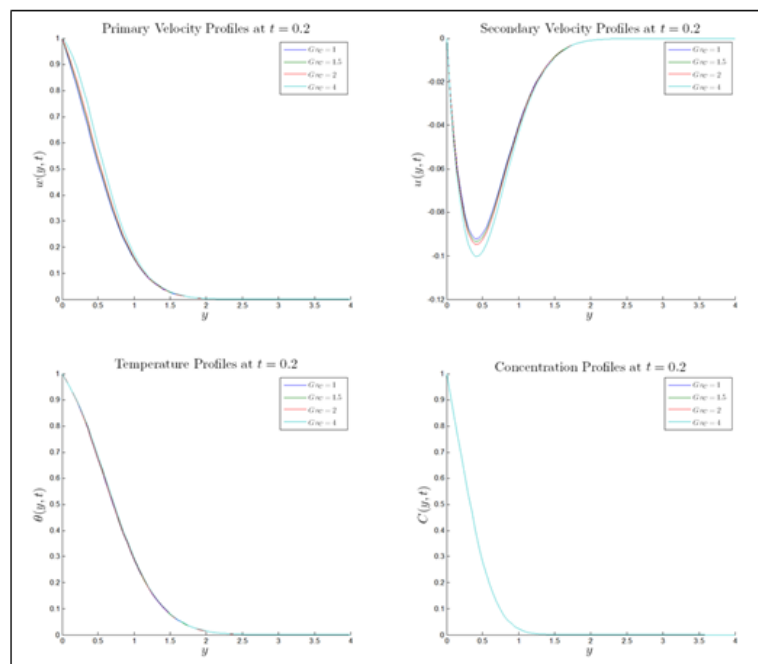


Figure 5: Flow profiles for various concentration Grashof numbers.

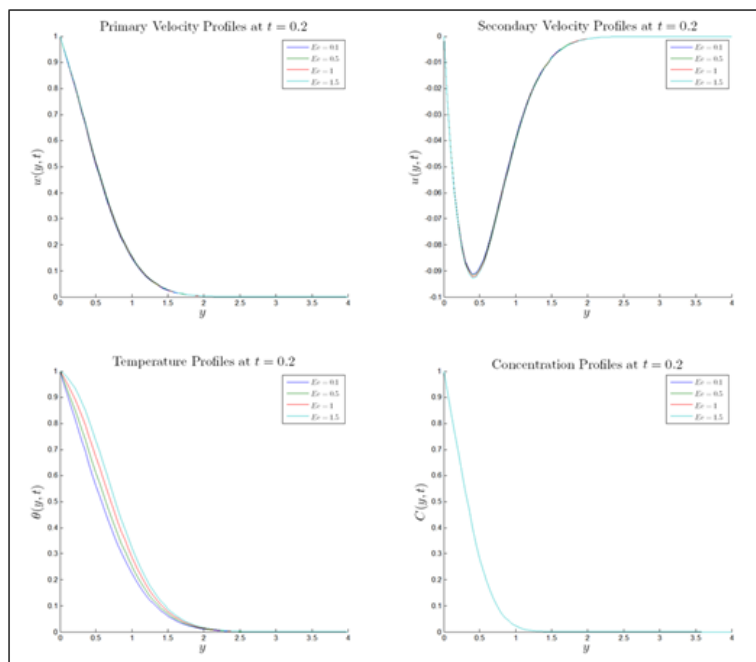


Figure 6: Flow profiles for various Eckert numbers.

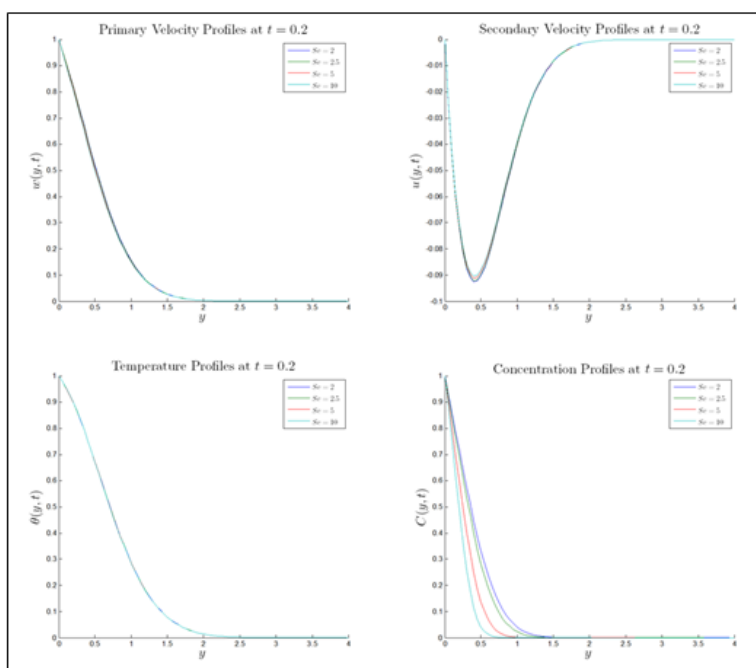


Figure 7: Flow profiles for various Schmidt numbers

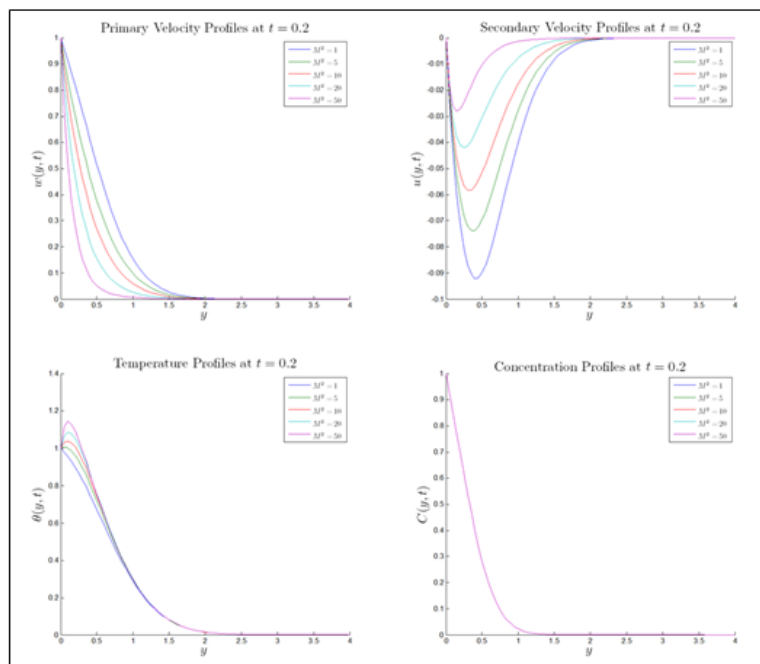


Figure 8: Flow profiles for various magnetic parameter values.

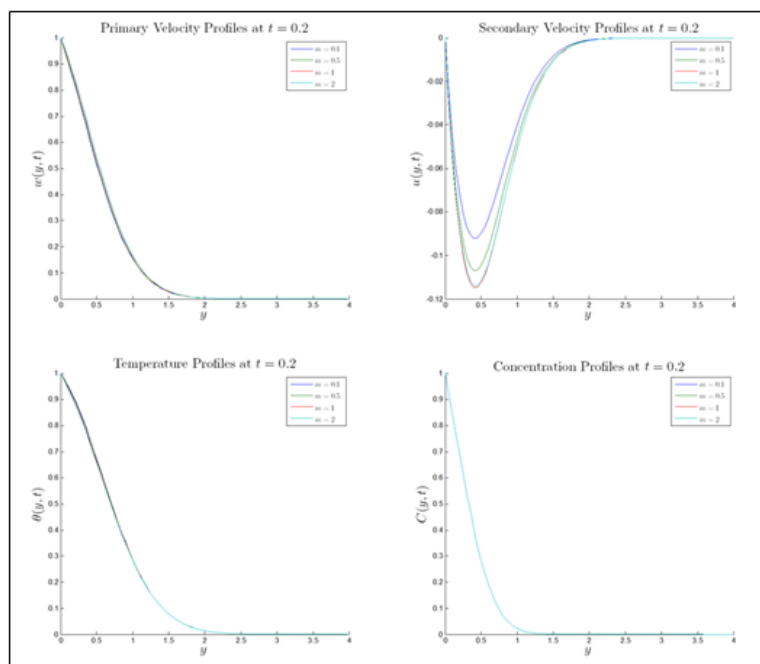


Figure 9: Flow profiles for various Hall parameter values.

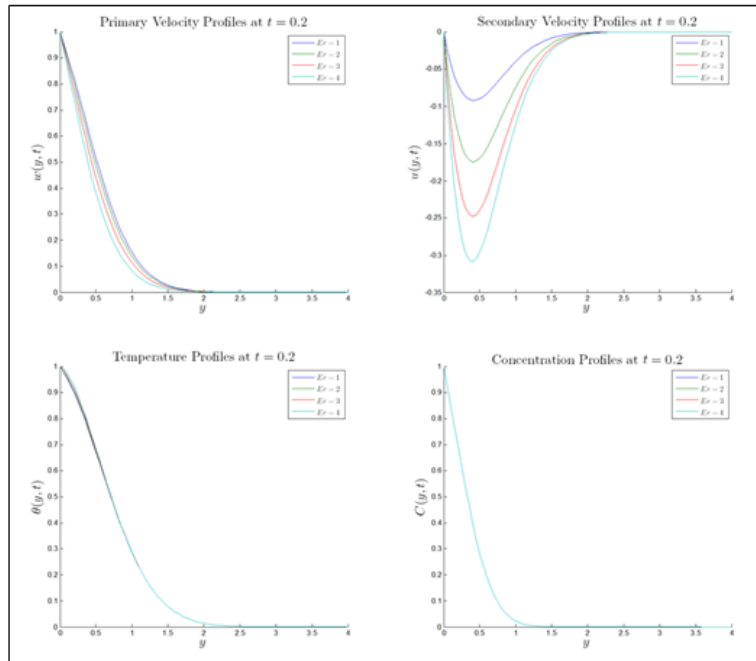


Figure 10: Flow variables for various rotational parameters.

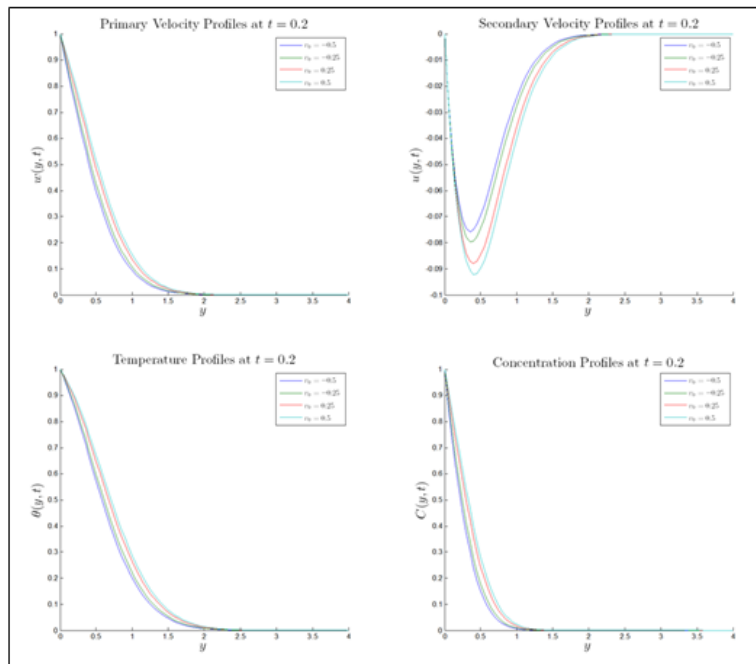


Figure 11: Flow profiles for various mass transfer velocities

6. Conclusion

The MHD problem in a rotating frame and porous medium has been solved with Hall currents, mass transfer, Joule's resistive heating and turbulence has been investigated. The present results compare well with those of Das *et al.* the results also follow physically expected trends. From the results obtained, we note the following:

- The primary velocity increases with $Gr_L > 0$ and $v_0 > 0$ but decreases with Pr , $Gr_L < 0$, M^2 , Er and $v_0 < 0$.
- The secondary velocity increases with $Gr_L > 0$, Gr_C , m , Er and $v_0 > 0$ but decreases with Pr , $Gr_L < 0$, M^2 and $v_0 < 0$.
- Temperature increases with Ec , M^2 and $v_0 > 0$ but decreases with Pr and $v_0 < 0$.
- Concentration increases with $v_0 > 0$ but decreases with Sc and $v_0 < 0$.

7. Future Scope of the Work

The approach here could be extended to factor in varying magnetic field and include the ion slip currents.

References

- [1] Prandtl, L. *On the motion of fluids of very small viscosity*. Verh. III. Intern. Math. Kongr., Heidelberg, S. 484-491, 1904.
- [2] Hartmann, J. *Theory of the laminar flow of an electrically conductive liquid in a homogeneous magnetic field*. K. Dan. Vidensk. Selsk. Mat. Fys. Medd. Vol. 15, issue 6, pg. 1-28, 1937.
- [3] Alfvén, H. *Existence of electromagnetic-hydrodynamic waves*. Nature, vol. 150, pg. 405-406, 1942.
- [4] Hasimoto, H. *Boundary Layer Growth on a Flat Plate with Suction or Injection*. Journal of Physical Society Of Japan vol. 12, pg 68-72, 1957.
- [5] Gupta, A. S. and Soundalgekar, V. M. *On Hydromagnetic Flow and Heat Transfer in a Rotating Fluid past an Infinite Porous Wall*. Zeitschrift fuer Angewandte Mathematik und Mechanik, vol. 55, pg. 762-764, 1975.
- [6] Mansuti, D., Pontrelli G and Rajagopal K. R. *Steady Flows of Non-Newtonian Fluids past a Porous Plate with Suction or Injection*. International Journal for Numerical Methods for Fluids vol. 17, pg. 927-941, 1993.
- [7] Kinyanjui, M., Chartuvedi N. and Uppal S. M. *MHD Stokes Problem for a Vertical Infinite Plate in a Dissipative Rotating Fluid with Hall Current*. Energy Conversion Management vol. 39, issue 5/6, pg. 541-548, 1998.
- [8] Sharma, P. R. and Pareek D. *Steady Free Convection MHD Flow past a Vertical Porous Moving Surface*. Indian Journal of Theoretical Physics vol. 50, pg 5-13, 2002.
- [9] Kwanza, J. K., Kinyanjui M. and Uppal S. M. *MHD Stokes Free Convection Flow past an Infinite Vertical Porous Plate Subjected to a Constant Heat Flux with Ion Slip Current and Radiation Absorption*. Far East Journal of Applied Mathematics vol. 12, issue 2, pg. 105-131, 2003
- [10] Makinde, O. D., Mango J. M. and Theuri D. M. *Unsteady Free Convection Flow with Suction on an Accelerating Porous Plate*. AMSE Journal of Modelling Measurement and Control B vol. 72, issue 3, pg. 39-46, 2003.
- [11] Chaudhar, R. C. and Jain A. *Combined Heat and Mass Transfer Effects on MHD Free Convection Flow past an Oscillating Plate Embedded in Porous Medium*. Romanian Journal of Physics vol. 52, issue 5, pg. 505-524, 2006.
- [12] Das, S. S., Satabathya A., Das J. K. and Sahoo S. K. *Numerical Solution of Unsteady Free Convective MHD Flow past an Accelerated Vertical Plate with Suction and Heat Flux*. Journal of Ultra Scientist of Physical Sciences vol. 19, issue pg. 105-112, 2007.
- [13] Ghosh, S and Ghosh A. K. *On Hydromagnetic Rotating Flow of a Dusty Fluid near a Pulsating Plate*. Computational and Applied Mathematics vol. 27, issue 1, pg. 1-30, 2008.
- [14] Das, S. S., Biswal S. R., Tripathy U. K. and Das P. *Mass Transfer Effects on Unsteady Hydromagnetic Convective Flow past a Vertical Porous Plate in a Porous Medium with Heat Source*. Journal of Applied Fluid Mechanics vol. 4, issue 4, pg. 91-100, 2011.
- [15] Mutua N., Kinyanjui M. and Kwanza J. *Stoke's Problem of a Convective Flow past a Vertical Infinite Plate in a Rotating System in Presence of Variable Magnetic Field*. International Journal of Applied Mathematics Research vol. 2, issue 3, pg. 5-11, 2013.
- [16] Del Sordo, F., Guerrero, G. and Brandenburg A. *Turbulent Dynamos with Advective Magnetic Helicity Flux*. Monthly Notices of the Royal Astronomical Society vol. 429, issue 2 pg 1686-1694, 2013.
- [17] McComb, W. D. *The Physics of Fluid Turbulence*. Oxford University Press, 1990.

Author Profile



Job Mayaka received his B.Ed (Science) and M.Sc. (Physics) in 2002 and 2010 from Maseno University and Kenyatta University respectively and currently a student at Pan African University Institute of Basic Sciences, Technology and Innovation. He has been a lecturer at Ol'lessos Technical Training Institute since 2010.



Johana Sigey is a Professor of Applied Mathematics at Jomo Kenyatta University of Agriculture and Technology. He is currently the deputy director, Kisii CBD Campus of Jomo Kenyatta University of Agriculture and Technology.



Mathew Kinyanjui is a Professor of Applied Mathematics and Fluid Mechanics at Jomo Kenyatta University of Agriculture and Technology. He is a former Chairman of the Department of Mathematics, now the School of Mathematics.